frontiers | Frontiers in Materials

TYPE Original Research
PUBLISHED 24 July 2023
DOI 10.3389/fmats.2023.1211129

OPEN ACCESS

EDITED BY
Xinmei Xiang,
Guangzhou University, China

REVIEWED BY
Li Xin,
Nanjing University of Science and Technology, China
Hongjian Du,
National University of Singapore, Singapore

*CORRESPONDENCE
Li Chen,
1063915947@qq.com

RECEIVED 24 April 2023
ACCEPTED 20 June 2023
PUBLISHED 24 July 2023

CITATION
Li J, Chen L, Luo J, Zhu W, Fan X, Zhu Y and Zhang Z (2023), Mechanical properties and microscopic characteristics of steel fiber coal gangue concrete.
Front. Mater. 10:1211129.
doi: 10.3389/fmats.2023.1211129

Mechanical properties and microscopic characteristics of steel fiber coal gangue concrete

Jiuyang Li[1], Li Chen[1]*, Jingwei Luo[1], Wenzhong Zhu[2], Xinmei Fan[1], Yuepeng Zhu[1] and Zicheng Zhang[3]

[1]School of Civil Engineering, Changchun Institute of Technology, Changchun, China, [2]School of Computing, Engineering and Physical Sciences, University of the West of Scotland, Scotland, United Kingdom, [3]China Construction First Group the Fifth Construction Co., Ltd., Shenzhen, China

Incorporation of coal gangue in the concrete mixes can realize utilization of the solid waste and reduce extraction/use of natural aggregates. To improve the mechanical properties of coal gangue concrete, this paper studies use of steel fibre together with coal gangue coarse aggregate, coal gangue fine aggregate/sand in various concrete mixes. The effect of volume dosages of steel fibre and different levels of replacing nature coarse aggregate and river sand with coal gangue aggregates on concrete compressive strength was first investigated. Then, a design of experiment using orthogonal test was adopted to study concrete mixes with 3 factors, namely, coal gangue coarse aggregate, coal gangue sand and steel fibre, and each at 3 levels. Through multidimensional statistical data analysis of the test results, the primary and secondary factors and the optimal composition of the steel fibre reinforced coal gangue concrete were identified, and a grey prediction model for compressive strength of the concrete mixes established. The microstructural characteristics and failure mechanism of steel fiber reinforced coal gangue concrete was also studied and discussed.

KEYWORDS

steel fiber, coal gangue, compressive strength, orthogonal test, microscopic mechanism, grey prediction model

1 Introduction

Hugh extraction and consumption of natural aggregate has brought a heavy burden to the ecological environment. At the same time, a large amount of coal gangue (Huang et al., 2018; Li and Wang, 2019; Yiran et al., 2020) is produced in process of coal mining. Due to its physical and chemical properties highly similar to those of natural aggregates, processed coal gangue coarse aggregate and coal gangue sand could partially replace natural coarse and fine aggregates to produce concrete (DUAN, 2014; Wang et al., 2020). However, due to its performance characteristics, use of coal gangue usually leads to a decrease in concrete strength. A number of relevant studies on using coal gangue in concrete have been carried out. Zhou M (Zhou et al., 2019) studied C30 concrete mixes with spontaneous combustion and non-spontaneous combustion coal gangue coarse aggregates to replace natural coarse aggregate at four replacement rates with 25% intervals. Microstructure, failure mode, and stress-strain curve of the coal gangue concrete mixes were studied. The results showed that peak strain increased, and peak stress decreased with increase in replacement rate. Yu L (Yu et al., 2022) prepared concrete (CGC) and mortar (CGM) with coal gangue to partially

substitute natural fine aggregates and studied the macroscopic and microscopic properties of CGC and CGM. It was reported that both CGC and CGM showed optimal properties at 25% coal gangue substitution rate. Huang Chengyang (Huang, 2015) also used coal gangue to replace natural coarse aggregate in concrete and reported that with a replacement rate of 60%, mechanical properties of concrete decreased by 26.8%. It was pointed out that a water-cement ratio lower than 0.4 should be used for preparation of strength grade C40 coal gangue concrete.

The damage mechanism of coal gangue concrete and plain concrete was comparatively analyzed by Benpei Chen (Chen, 1994) and Bing Yan (Yan, 2017), et al. It was found that for ordinary concrete damage occurred with cracks along the coarse aggregate edge/interface extending into mortar, while for coal gangue concrete, failure occurred with cracks directly penetrating through the coal gangue. In an attempt to improve mechanical properties of coal gangue concrete, Li J (Li et al., 2023) used different types of steel fibers in coal gangue concrete and studied their influence on mechanical properties of such concrete. It was concluded that shear steel fibers had the best improvement effect on concrete. Yang Qiuning et al. (Yang et al., 2023) studied the effects of steel fiber, polypropylene fiber, and polyvinyl alcohol fiber on the mechanical properties of coal gangue concrete at various fibre volume contents. It was reported that excessive content of polyvinyl alcohol fiber and polypropylene fiber could inhibit the strength of CGC, while steel fiber could improve the mechanical properties.

Based on the above research background, this study adopted the three-factor three-level orthogonal test method to investigate mechanical properties of concrete and analyze the damage mechanism from the microscopic level, so as to realize the "resourceful" utilization of coal gangue and provide a prediction model for optimization of such steel fibre reinforced coal gangue concrete mixes.

FIGURE 1
Steel fiber.

FIGURE 2
Coal gangue coarse aggregate.

2 Materials and concrete mixes used

2.1 Materials

Dinglu brand ordinary Portland cement (P.O 42.5), ordinary gravel of 5–20 mm, river sand with a fineness modulus of 2.6, and steel fiber with 40 mm in length and 1 mm in diameter were selected and used. The steel fibre having a tensile strength of 380–600 MPa is in Figure 1. Processed coal gangue coarse aggregate and coal gangue sand, as shown in Figures 2, 3, were provided by Chaoyang Hualong Co., Ltd. The composition and characteristics of the coal gangue products used are provided in Table 1.

2.2 Experimental design

A standard C30 concrete mix designed according to Chinese specification CECS 38:2004 (China Planning Press, 2004) and JGJ 55–2011 (China Architecture and Building Press, 2011a) was used as a starting point to study the effect of using coal gangue coarse aggregate, coal gangue sand and steel fibre on concrete performance. Mix proportions of such a control concrete mix are provided in Table 2, with its compressive strength verified by trials.

Based on the C30 control concrete mix, a large number of concrete mixes with varying levels of coal gangue coarse aggregate replacing gravel, coal gangue sand replacing river sand, as well as with different volume percentages of steel fibre were included in the experimental study. Cube compressive strength and axial compressive strength tests were carried out to study the mechanical performance of the concrete mixes.

(1) Parallel test: The effect of individual factors, namely, coal gangue coarse aggregate, coal gangue sand and steel fibre, on cube compressive strength of concrete mixes was studied. The results would allow a suitable percentage range of coal gangue coarse

FIGURE 3
Coal gangue sand.

aggregate, coal gangue sand and steel fibre to be determined for use in the orthogonal test below.

(2) Orthogonal test: A design of experiment using orthogonal test was adopted here to study concrete mixes with 3 factors, namely, coal gangue coarse aggregate, coal gangue sand and steel fibre, and each at 3 levels. Both cubic compressive strength (size: 100 mm × 100 mm × 100 mm) and axial compressive strength test (size: 150 mm × 150 mm × 300 mm) were conducted for this part of the study. Three specimens were made for each group. The results would lead to performance optimization of the steel fibre reinforced coal gangue concrete.

2.3 Specimen preparation and testing

According to the ratio and test quantity to calculate the number of various materials, weighing spare, test preparation procedures are as follows:

(1) Scrub and dry the required mold; Brush the dried mold with oil and label the number.
(2) Weigh all reserve materials, clean the mixer, and add water to moisten.
(3) Pour the pre-weighed fine aggregate, coal gangue ceramide, coal gangue ceramide sand, cement, steel fiber, and dry mix for 2 min.
(4) Pour the pre-weighed water and continue to stir for 3 min.
(5) The newly mixed concrete is poured into the mold and subsequently vibrated until the concrete is slurry, then the excess mix is scraped out with a spatula and the surface is trimmed.
(6) Leave for 24 h and then demold and maintain for 28 days.

2.4 Test method

This test was conducted according to the Chinese specification GB/T 50081-2019 (China Architecture and Building Press, 2019a). The loading equipment is an electro-hydraulic servo-hydraulic testing machine with a loading speed of 0.5 MPa/s and a maximum load accuracy of 0.01 Mpa.

Both cube compressive strength and axial compressive strength were obtained by dividing the maximum load value obtained from the test by the cross-sectional area of the specimen, multiplying it by a discount factor of 0.95, and analyzing the test results according to the test data processing method.

3 Results of the parallel test for studying individual factors

3.1 Cube compressive strength test

A number of studies (MeddahZitouniBelaabes, 2010; Yao et al., 2011; Cong et al., 2016; Wang et al., 2016; Gao et al., 2021) have been carried out to investigate the effect of using coal gangue aggregates and steel fiber individually on concrete performance. In this study, parallel test series for studying individual factors of coal gangue coarse aggregate, coal gangue sand and steel fibre on concrete performance were carried out in the first stage. The slump of concrete in the state of fresh mixing is between 50 and 140 mm. According to the provisions of the Chinese specification GB/T 50,164-2011 (China Architecture and Building Press, 2011b), the slump grade of the mixture is divided into S2-S3, which meets the requirements of engineering construction. Coal gangue coarse aggregate (CGL) was studied in the first series, where 10%, 20%, 30%, 40%, 50%, and 60% volumes of natural coarse aggregate were replaced by CGL. Similarly, coal gangue sand (CGS) was studied in the second series, where 10%, 20%, 30%, 40%, 50%, and 60% volumes of river sand were replaced by CGS. In the third series, steel fiber (SF) was studied with addition of 0.4%, 0.8%, 1.2%, 1.6%, and 2.0% of the volume of concrete. Brief code names for the concrete mixes in the form of "substituent-content" are used below in this paper. For example, CGL10 represents the mix having 10% coal gangue coarse aggregate replacing natural coarse aggregate; and SF04 represents the mix having 0.4% of steel fiber addition. The plain concrete control mix is corded as PC.

3.2 Analysis of cube compressive strength test results

Compressive strength using cube specimens was determined for all the concrete mixes in accordance with the Chinese standard JGJ/T 465-2019 (China Architecture and Building Press, 2019b). The strength results of the parallel test series are presented in Table 3 and plotted as bar-chart in Figure 4.

As the results shown in Table 3; Figure 4, For the use of coal gangue coarse aggregate, the cube compressive strength increased with CGL replacement level initially, reached a maximum at 30% CGL, below decreasing with further increase in CGL replacement.

TABLE 1 Main characteristics and composition of the coal gangue.

Particle size range	Density (kg/m^3)	Crushing index (%)	Porosity (%)	24 h water absorption (%)
0.5 ~ 4. (sand) 5 ~ 20 (oarse aggregate)	2,791	18.65	17.48	6.35
Color	SiO_2(%)	Al_2O_3(%)	Fe_2O_3(%)	Other (%)
Black	56.49	30.43	7.82	5.26

TABLE 2 Concrete mix design (unit: kg/m3).

Water cement ratio	Sand ratio	Water	Cement	Sand	Stone
0.60	40	220	366.67	725.33	1,087.99

For the use of coal gangue sand, the maximum cube strength was obtained with 20% CGS. For the addition of steel fiber, the cube compressive strength peaked at 0.8% SF.

As the gangue stiffness is less than natural aggregate, a small amount of substitution on the strength of concrete has a small effect, with the increase in substitution rate, the gangue ceramic particles under load crushing damage, the concrete strength decreased. When the number of steel fibers ≤0.8%, the steel fibers produce lap in the matrix, which inhibits the expansion of cracks, and the macroscopic performance of concrete strength is enhanced; when the amount of admixture continues to increase, more cement paste is needed to wrap the steel fibers, which reduces the compactness of concrete and causes the strength to decrease.

4 Results of orthogonal test of steel fiber reinforced coal gangue concrete

4.1 Design of experiment using orthogonal test

Use of orthogonal test can scientifically and rationally optimize the multi-factor and multi-level test scheme, reduce the number of tests, thus achieve the best test outcome with the minimum cost.

Based on the results of the parallel test above in Section 3, an orthogonal test with three factors, namely, A: coal gangue coarse aggregate content, B: coal gangue sand content and C: steel fibre content, and each at 3 levels was designed, as shown in Table 4.

4.1.1 Compressive strength results of the orthogonal test

After the standard curing for 28 days, the concrete specimens were tested for cube and axial compressive strength testing, with test setup and failure patterns shown in Figure 5. The standard deviation (σ) and coefficient of variation (CV) were calculated according to Eqs **1**, **2** and listed in Table 5 together with the test results.

$$\sigma = \sqrt{\frac{\sum (x - \bar{x})^2}{(n-1)}} \tag{1}$$

$$CV = \frac{\sigma}{\bar{x}} \tag{2}$$

According to the Chinese specification GB/T 50,081–2019 (China Architecture and Building Press, 2019a), it is known that the cube compressive strengths of the specimens are greater than 30 MPa and the axial compressive strengths are greater than 20.1 MP, and the coefficients of variation are less than 0.1, indicating that the test results are reliable.

4.2 Orthogonal test analysis

Using range analysis, variance analysis, and grey correlation analysis, the significance and priority of the influence of each factor on the mechanical properties of concrete can be analyzed. The grey model GM (1,4) was used to predict and analyze the test results, and the optimal combination of each factor and level and the strength prediction model were obtained.

4.2.1 Range analysis

4.2.1.1 Calculation method of range analysis

Range analysis method has the advantages of easy calculation, intuitive image, simple to understand, etc. It is the most commonly used method for the analysis of orthogonal test results. Its calculation formula is:

$$R_j = \max\left\{\overline{Y}_{j1}, \overline{Y}_{j2}, \cdots\right\} - \min\left\{\overline{Y}_{j1}, \overline{Y}_{j2}, \cdots\right\} \tag{3}$$

4.2.1.2 Range analysis results

Table 6 shows the results of the range analysis, with K1, K2, and K3 in the table being the average strengths of the three factors at three levels, respectively; R being the degree of influence of the level change of the factor on the strength, and the larger R indicates the greater the degree of influence of the factor on the compressive strength. To demonstrate more clearly the effects of different levels and factors on the cube compressive strength and axial compressive strength, the effect curve graph was drawn, as shown in Figure 6.

Results of Table 6; Figure 10 indicate that the importance of factors affecting the cube and axial compressive strength are: in descending order, coal gangue sand content, coal gangue coarse aggregate content, and steel fiber content. For each factor, the maximum value of K indicates the optimum combination. Thus, for the cubic compressive strength, the optimum combination is A2B2C2, that is, the coal gangue ceramics content of 30%, coal gangue ceramics sand content of 20%, and steel fiber content of 0.8%. For the axial compressive strength, the optimal combination is A2B1C2, that is, coal gangue ceramide content of 30%, coal gangue ceramide sand content of 10%, and steel fiber content of 0.8%.

With the increase in the amount of coal gangue coarse aggregate and coal gangue sand, the cubic compressive strength showed a

10.3389/fmats.2023.1211129

TABLE 3 Compressive strength results.

Specimen number	Compressive strength (MPa)	Specimen number	Compressive strength (MPa)	Specimen number	Compressive strength (MPa)
CGL10	33.12	CGS10	33.70	SF04	34.32
CGL20	33.65	CGS20	35.40	SF08	35.94
CGL30	34.55	CGS30	34.85	SF12	34.85
CGL40	33.80	CGS40	33.94	SF16	32.48
CGL50	32.52	CGS50	32.60	SF20	31.40
CGL60	31.40	CGS60	31.10	PC	32.64

trend of increasing first and then decreasing. The axial compressive strength showed a trend of increasing first and then stabilizing with the increase of coal gangue coarse aggregate, but showed a trend of increasing first and then decreasing with the increase in the amount of coal gangue sand. Such behaviors could be explained by the high water absorption and the relative weak strength of coal gangue particles. The water absorbed by the coal gangue particles could contribute to increased cement hydration due to the internal curing effect (Li et al., 2021). When the replacement rate is small, the internal curing effect of coal gangue is dominant, making the concrete strength rise. When the replacement rate of coal gangue particles reaches more than 40%, the negative impact of the weak coal gangue particles becomes dominant or comparable to the beneficial effect of internal curing, thus the concrete Compressive strength decreases or stablised. In addition, due to the coal gangue itself containing a large number of active SiO2, Al2O3, and it may lead to increase in long term strength due to potential pozzolanic action (Li et al., 2013; YangMiaoxiongLuo, 2013; Zhu et al., 2022).

Incorporating a small amount of steel fibers can improve the compressive strength of concrete, and it is known when the crack extends into the hardened cement paste, more energy needs to be consumed to pull the steel fibers across the crack, thus inhibiting the rapid expansion of the crack and increasing the strength and toughness of the specimen. However, as the amount of steel fibers increases, more slurry is needed to wrap the steel fibers in the mixing process, and due to the agglomeration/clustering effect of steel fibers, leading to increased porosity in such concrete mix, thus decreases the strength. But in general, the R-values of cubic compressive strength and axial compressive strength are the smallest under different levels of steel fiber addition, that is, the degree of influence of steel fiber addition on the performance of such steel fibre reinforced coal gangue concrete mixes is relatively small.

4.2.2 Variance analysis

4.2.2.1 Calculation method of variance analysis

Since the magnitude of the error cannot be estimated by the range analysis, it is necessary to test the degree of variation of the error for each group using the analysis of variance in addition to range analysis.

For $L_n(m^k)$ orthogonal table, its calculation method is as follows:

① Calculate total deviation sum of squares (SST) and total degrees of freedom (f_t)

$$SST = \sum_{i=1}^{n} x_i^2 - \frac{1}{n}\left(\sum_{i=1}^{n} x_i\right)^2 \tag{4}$$

$$f_T = n - 1 \tag{5}$$

② Calculate the sum of squares of deviation (SS_j) and degrees of freedom (f_j) for each column

$$SS_j = \frac{n}{m}\sum_{i=1}^{m}(t_i - \bar{x})^2 = \frac{m}{n}\sum_{i=1}^{m} T_i^2 - \frac{1}{n}\left(\sum_{i=1}^{n} x_i\right)^2 (j = 1, 2, \ldots, k) \tag{6}$$

$$f_j = m - 1 \tag{7}$$

③ Calculation error sum of squares (SSE) and degrees of freedom (f_e)

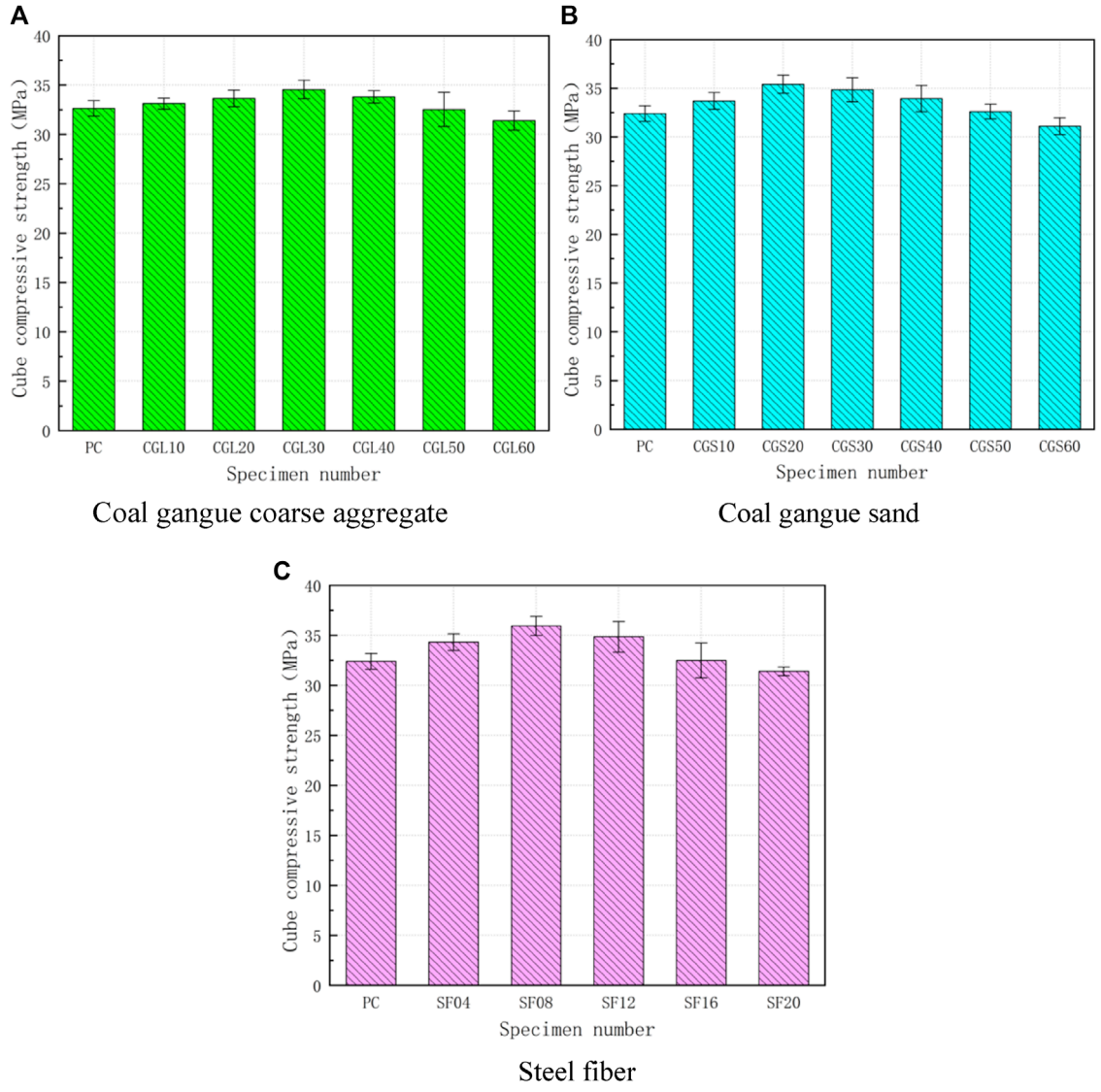

FIGURE 4
Cube compressive strength test results. **(A)** Coal gangue coarse aggregate **(B)** Coal gangue sand. **(C)** Steel fiber.

$$\mathrm{SSE} = \mathrm{SST} - \sum_{j=1}^{k} SS_j \tag{8}$$

$$f_e = f_T - \sum_{j=1}^{k} f_i \tag{9}$$

4.2.2.2 Variance analysis results

Variance analysis method was used to analyze the test results, the analysis results are shown in Table 7, the significance level was selected, and the critical value $F_{0.05}$ = 19 by the F distribution table to find the significance level of 0.05, the significance level of each factor of the test is less than $F_{0.05}$, indicating that each factor has a significant effect on the strength of concrete. The relative magnitude of the sum of squared deviation values for the different factors indicate that the degree of influence of coal gangue sand content > coal gangue coarse aggregate content > steel fiber content.

4.2.3 Grey correlation analysis

4.2.3.1 Calculation method of grey correlation analysis

The grey correlation analysis method can make up for the defects in mathematical statistics analysis and has no requirements on sample size and sample regularity. The basic idea is to determine whether the connection between different sequences is strong based on the similarity of the geometry of the sequence curves (Wu et al., 2022). The calculation process is as follows:

① The initial value transformation is performed on the original sequence

$$X_i = [x(1), x(2), \ldots, x(9)] \tag{10}$$

TABLE 4 Overview of orthogonal test.

Level	Factor		
	A:Coal gangue coarse aggregate content (%)	B:Coal gangue sand content (%)	C:Steel fiber content (%)
1	20	10	0.40
2	30	20	0.80
3	40	30	1.20

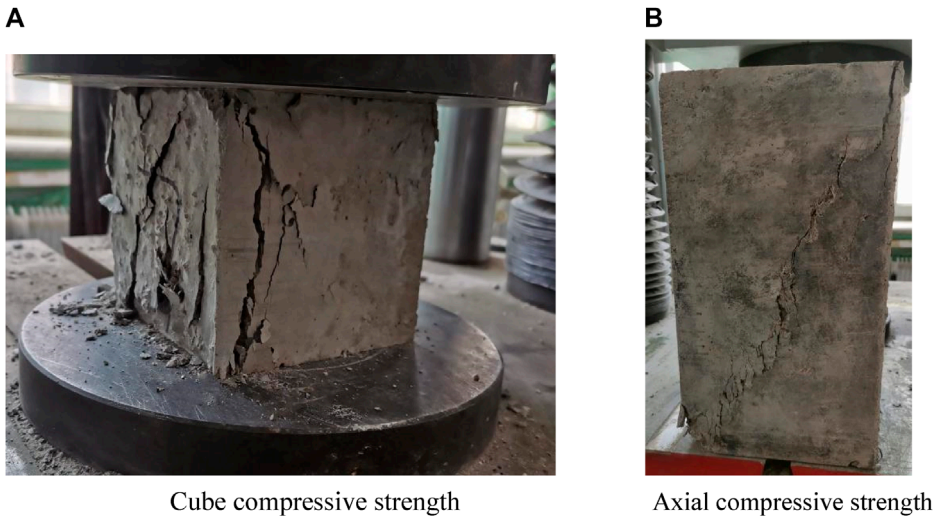

FIGURE 5
Test setup and failure patterns. **(A)** Cube compressive strength **(B)** Axial compressive strength.

TABLE 5 Orthogonal test result.

Specimen number	Cube compressive strength			Axial compressive strength		
	Strength value/MPa	Standard deviation/MPa	CV	Strength value/MPa	Standard deviation/MPa	CV
A1B1C1	34.83	1.86	0.05	29.80	1.31	0.04
A1B2C3	37.35	0.83	0.02	31.47	0.50	0.02
A1B3C2	34.76	1.35	0.04	29.98	0.62	0.02
A2B1C3	39.82	1.61	0.04	32.13	0.45	0.01
A2B2C2	38.05	0.41	0.01	32.02	0.48	0.01
A2B3C1	36.60	0.72	0.02	32.10	0.57	0.02
A3B1C2	35.96	1.75	0.05	34.56	1.02	0.03
A3B2C1	39.48	0.57	0.01	32.64	0.77	0.02
A3B3C3	32.15	1.69	0.05	29.16	1.16	0.04

$$Y_i = X_i D = [x(1)d, x(2)d, \ldots, x(9)d] \tag{11}$$

$$\mathrm{x}(k)d = \frac{x(k)}{x(k-1)}, \mathrm{x}(1)d = 1; \mathrm{k} = 2, 3, \ldots, n \tag{12}$$

Where, $X_i = (X_1, X_2, X_3, X_4)$ is the sequence of related factors, $x(1), x(2), \ldots, x(9)$ is the original sequence of the specimen about X_i, Y_i is the initial value vector after initializing X_i, D is the sequence operator, d is the elements of the sequence operator.

② Calculate the correlation coefficient matrix Z_i

$$Z_i = [\gamma_i(1), \gamma_i(2), \ldots, \gamma_i(9),], \mathrm{i} = 1, 2, 3, 4 \tag{13}$$

$$\gamma_i(k) = \left[\min_i \min_k |x_0(k) - x_i(k)| + \xi \max_i \max_j |x_0(k) - x_i(k)|\right] \left[|x_0(k) - x_i(k)| + \xi \max_i \max_j |x_0(k) - x_i(k)|\right]^{-1} \tag{14}$$

TABLE 6 Range analysis results of cube compressive strength and axial compressive strength.

Project	Cube compressive strength			Axial compressive strength		
	Coal gangue coarse aggregate content	Coal gangue sand content	Steel fiber content	Coal gangue coarse aggregate content	Coal gangue d content	Steel fiber content
K_1	35.65	36.87	36.30	30.42	32.83	31.51
K_2	38.16	39.29	37.59	32.12	32.71	32.19
K_3	35.86	34.50	36.44	32.08	30.08	30.92
R	2.51	4.79	1.29	1.67	2.75	1.27
Ranking of influencing factors	Coal gangue sand content > Coal gangue coarse aggregate content > Steel fiber content					

Where, Z_i is the correlation coefficient matrix, γ_i is the each column matrix of the correlation coefficient matrix, x_0, x_i is the sequence elements.

③ Calculate correlation

$$\gamma_i = \frac{1}{n}\sum_{k=1}^{n}\gamma_i(k) \tag{15}$$

4.2.3.2 Grey correlation analysis results

The strength index was defined as the behavior sequence X_0 of the system, and the gangue ceramic granule substitution rate, gangue ceramic sand substitution rate, and steel fiber doping were defined as the relevant factor sequences (X_1, X_2, X_3), and the raw data sequences obtained are shown in Table 8.

All series are initialized and the initial value vector Y is obtained. The initial value vector Y is put into Eq. **14** to establish the correlation coefficient matrix Z (as shown in Table 9) of the relevant sequence Y_i and the system characteristic behavior sequence Y_0. The correlation coefficient matrix Z is put into Eq. **15** for calculation. The correlation degree between the correlation factor sequence γ_i and the characteristic behavior sequence γ_0 of the system was obtained, as shown in Table 9.

From the analysis of Table 9, it can be seen that the correlation degree from large to small is as follows: coal gangue sand content, coal gangue coarse aggregate content, and steel fiber content. Analysis of the relationship between the significance of the correlation can be derived from the degree of influence of each factor. The extent of influence from strong to weak is coal gangue sand content, coal gangue coarse aggregate content, and steel fiber content, which is consistent with the results of range analysis and variance analysis.

4.2.4 Grey prediction model GM (1,4)

4.2.4.1 Calculation method of grey prediction model GM (1,4)

The general expression of the gray model (Liu and Guanghui, 2012; Prusty and Pradhan, 2020; Qiao et al., 2022) is GM(n, x), which means that the nth-order differential equation is used to model x variables. In this paper, we need to use the GM(1,4) model. The multivariate gray prediction model GM(1,4) is not a simple combination of GM(1,1), but an expansion of the GM(1,1) model under n elementary variables, and the main process of modeling is:

① The GM (1,4) model is established

$$\frac{dx}{dt} + ax_1 = b_1x_2 + b_2x_3 + b_3x_4 \tag{16}$$

Where, x_1, x_2, x_3, x_4 are respectively cube compressive strength/axial compressive strength, coal gangue ceramide content, coal gangue ceramic sand content and steel fiber content, a is the system development coefficient, b_1, b_2, b_3, b_4 is the driving coefficient

② Calculate the original sequence of GM (1,4) model

$$x_i^{(1)}(k) = \sum_{l=1}^{k} x_i^{(0)}(l) \tag{17}$$

Where, l is the number of specimen groups

10.3389/fmats.2023.1211129

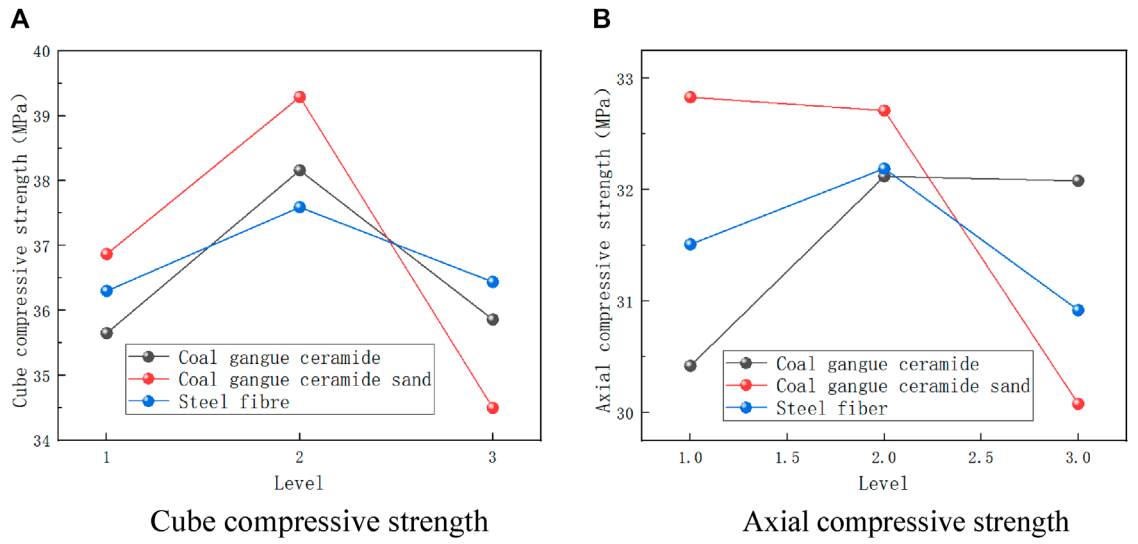

FIGURE 6
Range analysis effect curve. **(A)** Cube compressive strength **(B)** Axial compressive strength.

TABLE 7 Variance analysis results of cube compressive strength and axial compressive strength.

Dependent variable	Factor	SST	f_t	Mean square	F
Cube compressive strength	Coal gangue coarse aggregate content	17.91	2	8.95	8.95
	Coal gangue sand content	25.34	2	12.67	18.24
	Steel fiber content	3.41	2	1.70	2.45
Axial compressive strength	Coal gangue coarse aggregate content	6.18	2	3.09	5.55
	Coal gangue sand content	12.14	2	6.07	10.90
	Steel fiber content	2.92	2	1.46	2.62

TABLE 8 Steel fiber gangue concrete raw data series.

X_0		X_1	X_2	X_3
Cube compressive strength	Axial compressive strength			
34.83	29.80	0.20	0.10	0.004
37.35	31.47	0.20	0.20	0.012
34.76	29.98	0.20	0.30	0.008
39.82	32.13	0.30	0.10	0.012
38.05	32.02	0.30	0.20	0.008
36.60	32.10	0.30	0.30	0.004
35.96	34.56	0.40	0.10	0.008
39.48	32.64	0.40	0.20	0.004
32.15	29.16	0.40	0.30	0.012

TABLE 9 Correlation coefficient matrix of steel fiber coal gangue concrete and grey correlation.

	Cube compressive strength			Axial compressive strength		
	$\gamma_1(k)$	$\gamma_2(k)$	$\gamma_3(k)$	$\gamma_1(k)$	$\gamma_2(k)$	$\gamma_3(k)$
Correlation coefficient matrix	1.0000	1.0000	1.0000	1.0000	1.0000	1.0000
	0.5282	0.9349	0.3501	0.3421	0.9473	0.5171
	0.3415	0.9981	0.5089	0.5042	0.9939	0.3364
	0.8788	0.7443	0.3587	0.3446	0.7055	0.9283
	0.5336	0.7182	0.5336	0.5220	0.7038	0.5220
	0.3476	0.6981	0.9533	0.9220	0.7051	0.3445
	0.9697	0.5177	0.5177	0.5460	0.5460	0.8636
	0.5451	0.5451	0.8861	0.9138	0.5277	0.5277
	0.3333	0.4909	0.3333	0.3333	0.4974	0.3333
Grey correlation	0.609	0.739	0.605	0.604	0.736	0.597

③ Calculation system development coefficient (B) and driving term coefficient (â)

$$B = \begin{bmatrix} -0.5\left[X_1^{(1)}(1) + X_1^{(1)}(2)\right] & X_2^{(1)}(2) & \cdots & X_4^{(1)}(2) \\ -0.5\left[X_1^{(1)}(2) + X_1^{(1)}(3)\right] & X_1^{(1)}(3) & \cdots & X_4^{(1)}(3) \\ \vdots & \vdots & \ddots & \vdots \\ -0.5\left[X_1^{(1)}(8) + X_1^{(1)}(9)\right] & X_1^{(1)}(9) & \cdots & X_4^{(1)}(9) \end{bmatrix} \tag{18}$$

$$B = \begin{bmatrix} x_1^{(0)}(2) \\ x_1^{(0)}(3) \\ \vdots \\ x_1^{(0)}(9) \end{bmatrix} \tag{19}$$

$$\hat{a} = \begin{bmatrix} a & b_1 & b_2 & b_3 \end{bmatrix}^T \tag{20}$$

$$\hat{a} = \left(B^T B\right)^{-1} B^T Y \tag{21}$$

4.2.4.2 Grey prediction model GM (1,4) results

System development coefficient a and driving coefficient b_1, b_2, b_3, b_4 were calculated according to the method presented in the previous section, and the calculated values were put into Eq. **16** to obtain the gray prediction model of cube compressive strength as Eq. **22** and the gray prediction model of axial compressive strength as Eq. **23**

$$\frac{dx}{dt} + 2.0000x_1 = 0.6667x_2 + 0.6646x_3 + 0.6686x_4 \tag{22}$$

$$\frac{dx}{dt} + 2.0002x_1 = 0.6612x_2 + 0.6730x_3 + 0.6666x_4 \tag{23}$$

The accuracy of the model was determined by predicting and evaluating 9 groups of concrete specimens using Eqs **22**, **23**, and the results were examined by the residual test method. The results of the compressive strength of the cube and the axial compressive strength of the test values compared with the model predictions are shown in Table 10, and the test values and model predictions were plotted as in Figure 7.

Due to the errors in the specimen fabrication process as well as in the test process, the strength of the concrete specimens has a certain dispersion, and the test values in the middle grouping of Table 10 and Figure 7 have a large relative error with the model prediction. However, in summary, the average relative error of cubic compressive strength is 3.07%, and that of axial compressive strength is 3.06%, both of which are less than 5%, indicating that the prediction effect of the model is good.

5 Study on microstructure of steel fiber coal gangue concrete

When coal gangue ceramics, coal gangue ceramics sand, and steel fibers are added to concrete, the composition of a concrete matrix will change differently, thus forming a new interfacial transition zone. The material type, content, morphology, number of cracks and pores, and evolution of the transition zone at the interface of each material have an important influence on the mechanical properties of concrete.

At present, the research on gangue is mostly focused on the macroscopic level, and there are relatively few studies on the microscopic level. Therefore, in this paper, the microscopic morphology and failure forms of materials and the microscopic properties of different interfacial transition zones are further discussed through SEM observation.

5.1 Test overview

The scanning equipment is S-3400N scanning electron microscope. During the compressive strength test of concrete cubes with different mix ratios, samples meeting the scanning

10.3389/fmats.2023.1211129

TABLE 10 Comparison of experimental values and model predicted values.

specimen number	Cube compressive strength				Axial compressive strength			
	Experimental value (MPa)	Predicted value (MPa)	Residual error (MPa)	Relative error (%)	Experimental value (MPa)	Predicted value (MPa)	Residual error (MPa)	Relative error (%)
A1B1C1	34.83	34.83	0.00	0	29.80	29.80	0.00	0.00
A1B2C3	37.35	32.29	−5.05	13.53	31.47	27.21	−4.27	13.55
A1B3C2	34.76	38.49	3.74	10.75	29.98	33.12	3.13	10.45
A2B1C3	39.82	40.86	1.04	2.62	32.13	33.02	0.89	2.78
A2B2C2	38.05	38.28	0.23	0.60	32.02	32.21	0.19	0.60
A2B3C1	36.60	36.64	0.04	0.12	32.10	32.13	0.03	0.11
A3B1C2	35.96	35.97	0.01	0.02	34.56	34.57	0.01	0.03
A3B2C1	39.48	39.48	0.00	0.01	32.64	32.64	0.00	0.01
A3B3C3	32.15	32.15	0.00	0.01	29.16	29.16	0.00	0.01
Mean relative error (%)		3.07				3.06		

requirements of electron microscopy were selected from three different positions on the fracture surface of the specimen, and gold spraying was carried out by a plasma sputtering instrument. Then, the microstructural differences of the samples were analyzed by SEM, and the mechanism of action on the compressive strength of concrete was further analyzed.

5.2 Micromorphology and failure form of coal gangue

Figure 8 shows the microscopic morphology and failure forms of coal gangue particles. As can be seen from Figure 8A, there are a large number of micro-pores, and the overall structure is less dense than that of natural stone (Pan et al., 2006; DiZhangLiu, 2016). Particles of different sizes and shapes are distributed on the fracture surface, and the accumulation of these particles makes the internal structure of coal gangue low compactness. As shown in Figure 8B, hydration products fill relatively large voids inside the coal gangue particles, which can reduce its defects. Figure 8C showed a ruptured coal gangue coarse aggregate with cracks formed in the side and small coal gangue sand particles on the surface. The interface of the ceramic sand is relatively weak, so a large number of ceramic sand particles could be the cause of low coal gangue concrete strength.

5.3 Microstructure and failure form of steel fiber

Figure 9 shows the microscopic morphology of shear steel fiber mixed with concrete. The rough surface of the fibers effectively increases the cross-sectional area of the steel fibers, which increases the bonding effect between the fibers and the concrete matrix, thus improving the strength of the concrete. The distribution of hydration product particles on the surface of the fiber also confirms the above situation. The steel fibers bear the external load together with the concrete matrix through adhesion and bridging, absorbing large amounts of energy while effectively inhibiting the extension and expansion of cracks and improving the strength of the concrete.

5.4 Microstructure of different interfaces

The interface transition zone has a large impact on the performance of cementitious materials (Cwirzen and Penttala, 2005). Therefore, in this section, microstructural examinations of the gangue-cement paste interface transition zone, aggregate-cement paste interface transition zone, and steel fiber-cement paste interface transition zone were conducted.

5.4.1 Microstructure of aggregate-cement paste ITZ

As can be seen from Figure 10, there is a lot of C-S-H, CH, AFt, and other substances in the ITZ (interfacial transition zone) of aggregate-cement paste. These crystals form a contact layer at the intersection of the aggregate and the cement paste, i.e., the interfacial transition zone (ITZ). Due to the volcanic ash effect of coal gangue, more AFt crystals and C-S-H gels are produced with the constant

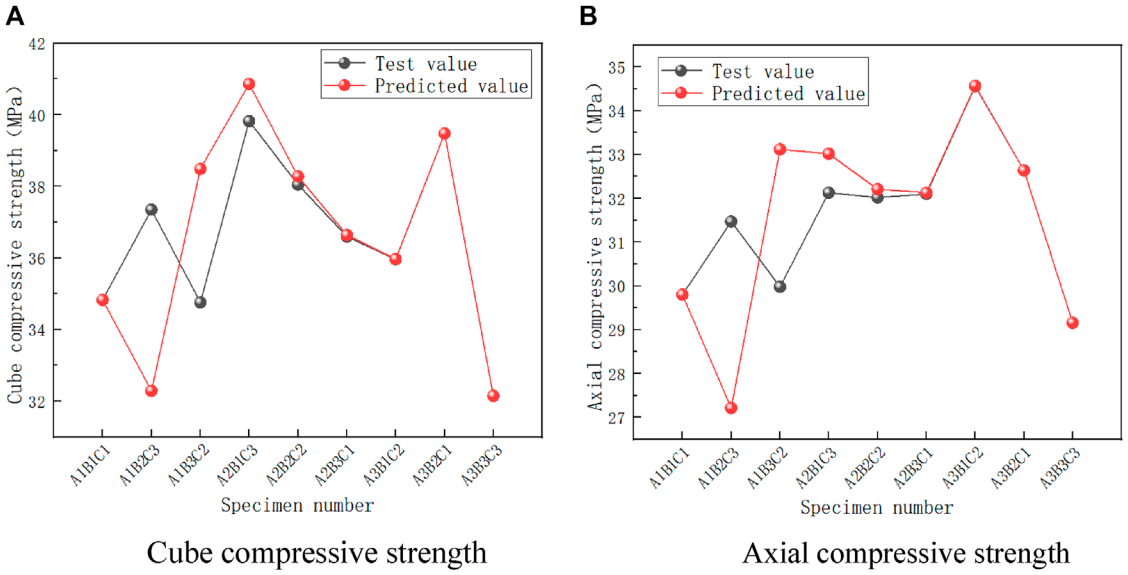

FIGURE 7
Comparison of experimental values and model predicted values. **(A)** Cube compressive strength **(B)** Axial compressive strength.

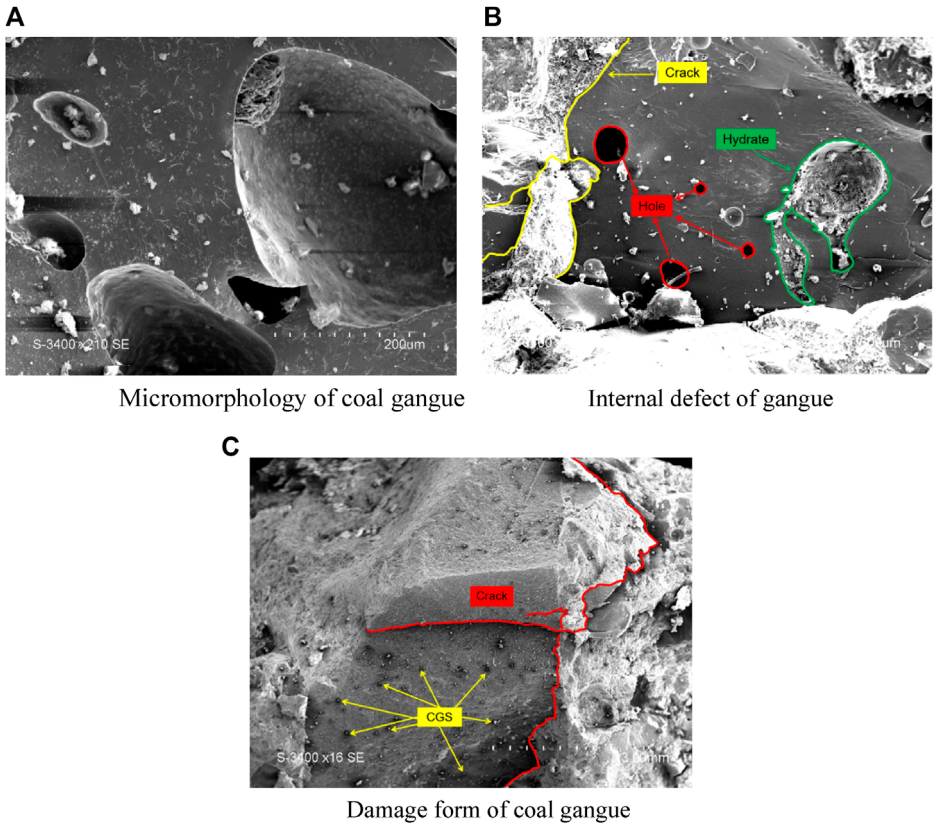

FIGURE 8
Micromorphology and failure form of coal gangue. **(A)** Micromorphology of coal gangue **(B)** Internal defect of gangue. **(C)** Damage form of coal gangue.

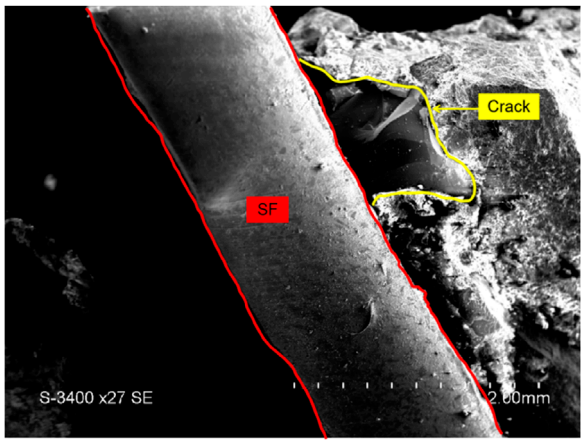

FIGURE 9
Microstructure and failure form of steel fiber.

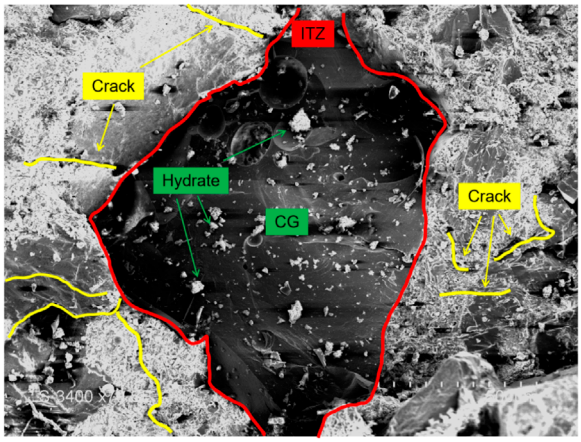

FIGURE 11
ITZ of coal gangue—cement slurry.

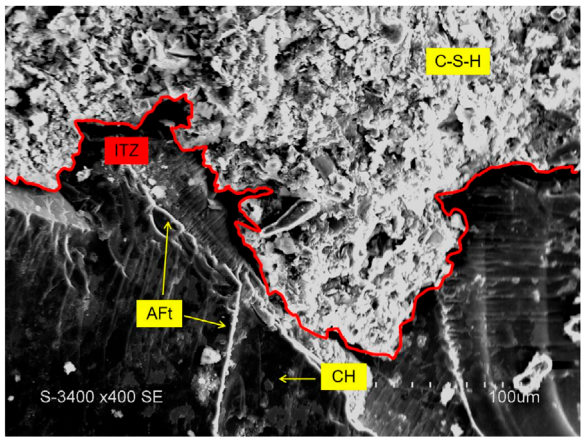

FIGURE 10
ITZ of aggregate—cement paste.

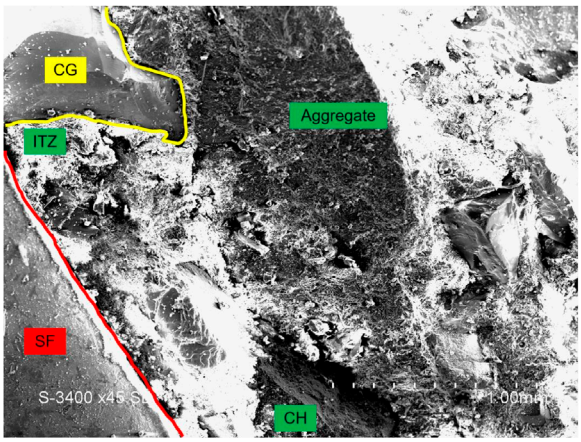

FIGURE 12
ITZ of steel fiber-cement slurry-coal gangue interface.

consumption of CH crystals in the hydration reaction. When the CH crystals reach a certain amount, they are precipitated in the form of layered accumulation, and AFt and C-S-H are intertwined, thus reducing the specific surface area and molecular binding force, so the boundary of the ITZ area is prone to cracks, and the strength of the concrete is reduced (Xie et al., 1996). In addition, C-S-H gel has large pores, low friction, and bonding force, resulting in a loose overall structure inside the concrete, a large number of holes in the matrix, and some cracks and "voids" formed by external force damage and other reasons, and poor overall compactness. The existence of these microscopic defects harms mechanical properties.

5.4.2 Microstructure of coal gangue-cement paste ITZ

According to the SEM image of the transition zone between coal gangue and cement paste in Figure 11, it can be seen that there are many hydration products of different sizes attached to the surface of coal gangue (CG), and many cracks, holes, and incomplete substances can still be observed on the surface of the matrix. With the increase in curing time, coal gangue and other small particles participate in hydration more thoroughly, and hydration products also increase. The flocculent gel generated by hydration expands continuously with the deepening of the hydration process, which can fill part of the original small holes and cracks and connect the materials in the matrix, and the macro performance is the increase of the strength of concrete. In addition, the irregular surface of the crushed coal gangue increases the covering area of the cement slurry and improves the compressive strength of concrete to a certain extent.

5.4.3 Microstructure of steel fiber-cement paste-gangue ITZ

From the SEM image of the steel fiber-cement paste-coal gangue interfacial transition zone in Figure 12, the distribution of the material can be seen. Compared with other ITZ, the range of steel fiber-cement paste-coal gangue ITZ is smaller, mainly because the

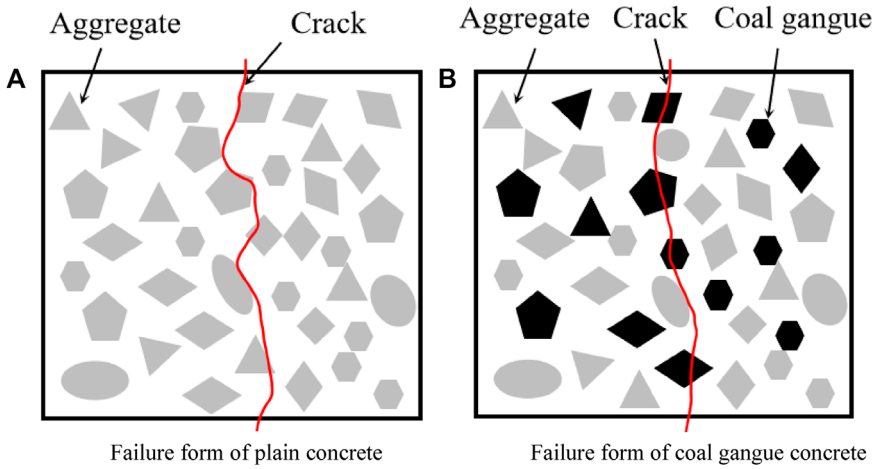

FIGURE 13
Comparison of concrete failure forms. **(A)** Failure form of plain concrete **(B)** Failure form of coal gangue concrete.

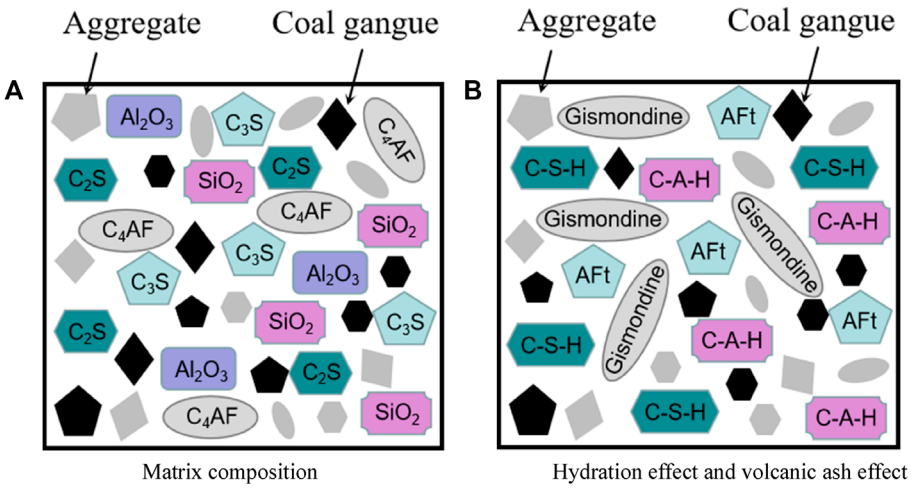

FIGURE 14
Schematic diagram of reinforcement mechanism model for coal gangue. **(A)** Matrix composition **(B)** Hydration effect and volcanic ash effect.

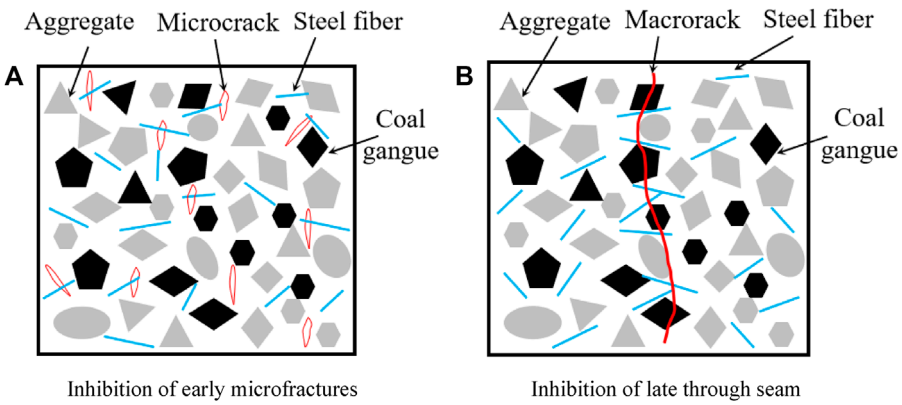

FIGURE 15
Schematic diagram of steel fiber reinforced mechanism model. **(A)** Inhibition of early microfractures **(B)** Inhibition of late through seam.

randomly distributed steel fibers overlap each other in the matrix to form a skeleton, prevent the sinking of the aggregate, and enhance the performance of ITZ. In addition, ITZ between aggregate, coal gangue, and steel fiber is visible. Flocculent C-S-H gel is distributed around steel fiber and coal gangue, and flake CH and acicular AFt are distributed around the gel. These substances can bond well with steel fiber. When steel fiber is destroyed, more energy is consumed, and a certain toughening effect is achieved.

5.5 Failure form and reinforcement mechanism of steel fiber and coal gangue to concrete

5.5.1 Failure forms of coal gangue concrete

For plain concrete, the elastic modulus of aggregate is higher than that of mortar, and the junction between mortar and aggregate is a weak link. There are primary cracks here. When concrete is subjected to load, the load is transferred along the weak interface between aggregate and mortar, and the primary cracks continue to expand along the periphery of aggregate and extend into the mortar. As shown in Figure 13A. For gangue concrete, its failure form is different from that of plain concrete. As the elastic modulus of gangue aggregate is lower than that of mortar, when the stress increases, cracks will not only expand along the interface between aggregate and mortar but also run through the gangue aggregate, as shown in Figure 13B.

5.5.2 Reinforced mechanical structure model of coal gangue

Through SEM study, the reinforcement effect of gangue concrete is mainly composed of the hydration effect of Portland cement and the pozzolanic effect of gangue. Tricalcium silicate (C_3S), dicalcium silicate (C_2S), tricalcium aluminate (C_3A), terrarium-aluminum ferrite (C_4AF) in common Portland cement and aluminum oxide (Al_2O_3), and silica (SiO_2) in coal gangue, as shown in Figure 14A. Dense AFt crystals and C-S-H and C-A-H gels were formed by hydration reaction respectively, and gismondine was generated by volcanic ash effect, as shown in Figure 14B. AFt crystal and C-S-H gel can be attached to the surface of the gelled material, slowing down the reaction rate of the active ingredients in the matrix and the consumption rate of calcium hydroxide crystals, so that the hydration reaction is more thorough, and more gismondine crystals are generated, showing good compressive properties on the macro level.

5.5.3 Structural model of steel fiber reinforced mechanism

The steel fibers are randomly distributed in the concrete matrix and form a three-dimensional skeleton together with the paste and aggregate, which can inhibit crack expansion at different stages of crack development. When subjected to external loads, microcracks appear inside the matrix, and the steel fibers across the cracks can inhibit shrinkage, resulting in fewer shrinkage cracks in the concrete, as shown in Figure 15A. With the increasing load, the internal micro-cracks will produce concentrated stress on the surface of the gangue after development, causing damage to the gangue and producing through cracks as shown in Figure 15B. When an appropriate amount of steel fibers is added to the matrix, the steel fibers are cross-distributed on the damaged surface of the gangue concrete, which can uniformly transfer the stress as well as anchor the concrete, and more energy needs to be consumed to pull off or pull out the steel fibers, thus reducing the damage to the gangue particles, which is macroscopically expressed as an increase in the compressive strength of the steel gangue concrete.

6 Conclusion

Through the use of the parallel test and orthogonal test, the effect of coal gangue coarse aggregate replacement level, coal gangue sand replacement level and steel fiber addition dosage on mechanical performance of steel fibre reinforced coal gangue concrete were studied, together with a limited the microstructure observation-theoretical analysis, The following conclusions could be drawn:

(1) Through range analysis, variance analysis, and gray correlation analysis of the different factors on the concrete cube compressive strength, axial compressive strength, the degree of significance of the factors could be ranked as: coal gangue sand content > coal gangue coarse aggregate content > steel fiber content.
(2) The optimum composition obtained by the comprehensive analysis of the orthogonal test is 30% coal gangue coal gangue coarse aggregate content, 10%–20% coal gangue sand content, and 0.8% steel fiber content.
(3) Through the fitting analysis of the grey prediction model GM (1,4) for the orthogonal test results, the grey prediction model of the cube compressive strength and the axial compressive strength of steel fiber coal gangue concrete was obtained. According to this model, materials with different mix ratios can be predicted within a certain range (20%–40% coal gangue ceramide, 10%–30% coal gangue ceramide sand, 0.4%–0.8% steel fiber content).
(4) Due to the low elastic modulus of coal gangue itself, the strength of the matrix decreases. After adding steel fiber, the network structure system of coal gangue—fiber—aggregate—cement slurry can delay the expansion rate of cracks. The Gismondine generated by volcanic ash activity of coal gangue and the C-S-H gel generated by hydration is nested with AFt crystals. The pores are filled, the adhesion of the interface is improved, and the internal compactness of the concrete is enhanced, so that the system has a higher strength.

Data availability statement

The original contributions presented in the study are included in the article/Supplementary material, further inquiries can be directed to the corresponding author.

Author contributions

JLi: financial support, conceptualization, formal analysis, writing—review and editing. LC: original draft, specimen production, formal analysis. JLu: specimen production, formal

analysis, formal analysis. XF: project administration, YZ: methodology. ZZ: formal analysis. All authors contributed to the article and approved the submitted version.

Conflict of interest

Author ZZ was employed by China Construction Fifth Engineering Division Corp., Ltd., China.

The remaining authors declare that the research was conducted in the absence of any commercial or financial relationships that could be construed as a potential conflict of interest.

Publisher's note

All claims expressed in this article are solely those of the authors and do not necessarily represent those of their affiliated organizations, or those of the publisher, the editors and the reviewers. Any product that may be evaluated in this article, or claim that may be made by its manufacturer, is not guaranteed or endorsed by the publisher.

References

Chen, Benpei (1994). Strength of coal gangue concrete. *Ind. Build.* (7), 29–32+42.

China Architecture and Building Press, (2019a). *GB/T 50081-2019, Test method standard for physical and mechanical properties of concrete*. Beijing, China: China Architecture and Building Press.

China Architecture and Building Press, (2011b). *GB/T 50164-2011, concrete quality control standard*. Beijing, China: China Architecture and Building Press.

China Architecture and Building Press, (2011a). *JGJ 55-2011, General Concrete mix design code*. Beijing, China: China Architecture and Building Press.

China Architecture and Building Press, (2019b). *JGJ/T 465-2019, steel fiber reinforced concrete structure design standard*. Beijing, China: China Architecture and Building Press.

China Planning Press, (2004). *CECS 38:2004, technical specification for fiber reinforced concrete structures*. Beijing, China: China Planning Press.

Cong, X. Y., Lu, S., Yao, Y., and Wang, Z. (2016). Fabrication and characterization of self-ignition coal gangue autoclaved aerated concrete. *Mater. Des.* 97, 155–162. doi:10.1016/j.matdes.2016.02.068

Cwirzen, A., and Penttala, V. (2005). Aggregate–cement paste transition zone properties affecting the salt–frost damage of high-performance concretes. *Cem. Concr. Res.* 35 (4), 671–679. doi:10.1016/j.cemconres.2004.06.009

DiZhangLiu, W. Y. Y. (2016). Mechanical performance and ultrasonic properties of cemented gangue backfill with admixture of fly ash. *Ultrasonics* 64, 89–96. doi:10.1016/j.ultras.2015.08.004

Duan, X. M. (2014). *Study on microstructure and physical and mechanical properties of coal gangue aggregate concrete*. Beijing, China: China University of Mining and Technology.

Gao, D., Gu, Z., Pang, Y., and Yang, L. (2021). Mechanical properties of recycled fine aggregate concrete incorporating different types of fibers. *Constr. Build. Mater.* 298, 123732. doi:10.1016/j.conbuildmat.2021.123732

Huang, C. Y. (2015). *Research on impermeability and frost resistance of concrete with coal gangue replacing coarse aggregate*. Shenyang, China: Shenyang Jianzhu University.

Huang, G., Ji, Y., Li, J., Hou, Z., and Dong, Z. (2018). Improving strength of calcinated coal gangue geopolymer mortars via increasing calcium content. *Constr. Build. Mater.* 166, 760–768. doi:10.1016/j.conbuildmat.2018.02.005

Li, J., Chen, L., Wang, X., Hu, G., Wang, Z., Guo, J., et al. (2023). Effect of compounding conductive materials on the mechanical properties of concrete and the microscopic mechanism. *Constr. Build. Mater.* 377, 131000. doi:10.1016/j.conbuildmat.2023.131000

Li, J., and Wang, J. (2019). Comprehensive utilization and environmental risks of coal gangue: A review. *J. Clean. Prod.* 239, 117946. doi:10.1016/j.jclepro.2019.117946

Li, J., Zhao, E., Niu, J., and Wan, C. (2021). Study on mixture design method and mechanical properties of steel fiber reinforced self-compacting lightweight aggregate concrete. *Constr. Build. Mater.* 267, 121019. doi:10.1016/j.conbuildmat.2020.121019

Liu, Feng, and Guanghui, W. E. I. (2012). Fuzzy optimization of hydraulic engineering scheme based on grey correlation. *J. Hydropower* 31 (1), 10–14+26.

Li, Y., Yao, Y., Liu, X., Sun, H., and Ni, W. (2013). Improvement on pozzolanic reactivity of coal gangue by integrated thermal and chemical activation. *Fuel* 109, 527–533. doi:10.1016/j.fuel.2013.03.010

MeddahZitouniBelaabes, M. S. S. (2010). Effect of content and particle size distribution of coarse aggregate on the compressive strength of concrete. *Constr. Build. Mater.* 24 (4), 505–512. doi:10.1016/j.conbuildmat.2009.10.009

Pan, G. Z., Song, X., Gong, C., and Pan, Z. (2006). Research on cementitious behavior and mechanism of pozzolanic cement with coal gangue. *Cem. Concr. Res.* 36, 1752–1759. doi:10.1016/j.cemconres.2004.11.004

Prusty, J. K., and Pradhan, B. (2020). Multi-response optimization using Taguchi-Grey relational analysis for composition of fly ash-ground granulated blast furnace slag based geopolymer concrete. *Constr. Build. Mater.* 241, 118049. doi:10.1016/j.conbuildmat.2020.118049

Qiao, Lidong, Yao, Zhanquan, Wang, Zongxi, Zhang, Zijian, and He, Liang (2022). Grey entropy analysis of coal gangue on macro and micro properties of concrete. *J. Drainage Irrigation Mach. Eng.* 40 (1), 30–34+54.

Wang, J., Qin, Q., Hu, S., and Wu, K. (2016). A concrete material with waste coal gangue and fly ash used for farmland drainage in high groundwater level areas. *J. Clean. Prod.* 112, 631–638. doi:10.1016/j.jclepro.2015.07.138

Wang, Q., Li, Z., Zhang, Y., Zhang, H., Zhou, M., and Fang, Y. (2020). Influence of coarse coal gangue aggregates on elastic modulus and drying shrinkage behaviour of concrete. *J. Build. Eng.* 32, 101748. doi:10.1016/j.jobe.2020.101748

Wu, Hailin, Guo, Jinyu, and Zhang, Yu (2022). Orthogonal test on compressive strength of hybrid fiber reinforced concrete. *Sci. Technol. Eng.* 22 (32), 14370–14378.

Xie, P., Gu, P., and Beaudoin, J. J. (1996). Electrical percolation phenomena in cement composites containing conductive fibres. *J. Mater. Sci.* 31 (15), 4093–4097. doi:10.1007/bf00352673

Yan, Bing (2017). *Experimental study on mechanical properties and frost resistance of modified coal gangue aggregate concrete*. Xi'an, China: Xi 'an University of Architecture and Technology.

Yang, Qiuning, Jing, Yanyi, and Zhang, Dongsheng (2023). Study on mechanical properties of coal gangue concrete modified by fiber and mineral admixture. *J. Funct. Mater.* 202 (7), 7150–7156.

YangMiaoxiongLuo, Q. L. Y. (2013). Effects of surface-activated coal gangue aggregates on properties of cement-based materials. *J. Wuhan Univ. Technol.* 28 (6), 1118–1121. doi:10.1007/s11595-013-0830-2

Yao, Y., Wu, H., and Wang, L. (2011). The microstructure research on interfacial transition zone of filling material containing fa and coal gangue. *Adv. Mater. Res.* 287, 1125–1129. doi:10.4028/www.scientific.net/amr.287-290.1125

Yiran, T., Xiaoran, Z., Junfeng, L., Kaihong, S., Ziyang, Z., Chaohong, T., et al. (2020). Research progress of coal gangue recycling as environmental materials. *Sci. Technol. Rev.* 38 (22), 104–113.

Yu, L., Xia, J., Xia, Z., Chen, M., Wang, J., and Zhang, Y. (2022). Study on the mechanical behavior and micro-mechanism of concrete with coal gangue fine and coarse aggregate. *Constr. Build. Mater.* 338, 127626. doi:10.1016/j.conbuildmat.2022.127626

Zhou, M., Dou, Y., Zhang, Y., and Zhang, B. (2019). Effects of the variety and content of coal gangue coarse aggregate on the mechanical properties of concrete. *Constr. Build. Mater.* 220 (30), 386–395. doi:10.1016/j.conbuildmat.2019.05.176

Zhu, M., Qiu, J., and Chen, J. (2022). Effect and mechanism of coal gangue concrete modification by basalt fiber. *Constr. Build. Mater.* 328, 126601. doi:10.1016/j.conbuildmat.2022.126601